

# Journal of Biomedical Optics

[SPIEDigitalLibrary.org/jbo](http://SPIEDigitalLibrary.org/jbo)

## **Simulating the scanning of a focused beam through scattering media using a numerical solution of Maxwell's equations**

Ahmed Elmaklizi  
Jan Schäfer  
Alwin Kienle

# Simulating the scanning of a focused beam through scattering media using a numerical solution of Maxwell's equations

Ahmed Elmaklizi,\* Jan Schäfer, and Alwin Kienle

Institut für Lasertechnologien in der Medizin und Meßtechnik an der Universität Ulm, Helmholtzstr.12, D-89081 Ulm, Germany

**Abstract.** A highly efficient method based on Maxwell's theory was developed, which enables the calculation of the scanning of a focused beam through scattering media. Maxwell's equations were numerically solved in two dimensions using finite difference time domain simulations. The modeling of the focused beam was achieved by applying the angular spectrum of plane waves method. The scanning of the focused beam through the scattering medium was accomplished by saving the results of the near field obtained from one simulation set of plane waves incident at different angles and by an appropriate post processing of these data. Thus, an arbitrary number of focus positions could be simulated without the need to further solve Maxwell's equations. The presented method can be used to efficiently study the light propagation of a focused beam through scattering media which is important, for example, for different kinds of scanning microscopes. © 2014 Society of Photo-Optical Instrumentation Engineers (SPIE) [DOI: [10.1117/1.JBO.19.7.071404](https://doi.org/10.1117/1.JBO.19.7.071404)]

Keywords: focus; phase shifts; spatial light modulators; tomography; multiple scattering; scanning; scanning microscopy.

Paper 130705SSR received Sep. 27, 2013; revised manuscript received Nov. 26, 2013; accepted for publication Dec. 9, 2013; published online Jan. 6, 2014; corrected Jan. 15, 2014.

## 1 Introduction

High-resolution microscopy has been an important research topic for a long time due to its applications in many fields in science, industry, and especially, biomedical optics. Many of the high-resolution microscopy techniques like confocal microscopy,<sup>1</sup> two-photon microscopy,<sup>2,3</sup> and optical coherence tomography<sup>4</sup> depend on focusing of the illuminating light into a tight spot at the point of interest. The focusing of the beam has the advantage of increasing the resolution of the microscope but it increases the measurement time, since it becomes necessary to scan the focus in order to get a full image of the considered sample. Accordingly, to simulate the interaction between a scattering sample and the incident scanning light beam, the simulation needs, in principle, to be run for every position of the scanned focus. This can be extremely time consuming depending on the type of simulator used. In this work, an efficient technique is introduced, which models the scanning of a beam through a scattering medium using the finite difference time domain (FDTD) method.

Experimentally, it is possible to achieve the scanning of a focused beam for example by using spatial light modulators (SLMs). SLMs are opto-electronic devices that modulate the amplitude or the phase of a beam of light. These devices are often used in order to shape the wave front of the light.<sup>5,6</sup> This is done in all sorts of fields from astronomy to microscopy. The phase of each pixel on the SLM can be modified digitally to shift the beam.<sup>7</sup>

In a previous study, focused beams have been modeled with the FDTD method using the angular spectrum of plane waves approach (ASPW).<sup>8,9</sup> This method has been used to study the

scattering of a focused beam by biological tissue<sup>10</sup> and to investigate optical projection tomographic microscopy.<sup>11</sup>

In this work, the ASPW method is used to model the incident focused light as a summation of plane waves in two dimensions. Then, the method of scanning the focused beam based on the addition of an extra phase to the calculated near fields caused by each individual plane wave is introduced. This method allows the beam to be shifted without the need to re-simulate the beam propagation again. Thus, the calculation time is strongly reduced at the expense of larger memory requirements. Results are shown for both axial and lateral scans. The calculations are carried out using FDTD simulations, which allow to accurately model plane waves with oblique angles relative to the optical axis. The self-implemented FDTD simulation tool is verified in both the near- and far-field domains by comparing the results with analytical solutions<sup>12</sup> using both plane waves and focused beams as incident light.

## 2 Theory

In this section, the developed FDTD simulation tool is discussed. Then the ASPW method is described mathematically, followed by its usage in modeling a focused beam in two dimensions. After that the basis of the beam scanning is shown.

### 2.1 Finite Difference Time Domain Method

The numerical technique that has been used in this work to solve Maxwell's equations is the FDTD method, which offers a solution for complex scattering geometries.<sup>13</sup> The developed code was implemented using MATLAB. The injection of the incident beam is achieved using the total-field/scattered-field method (TF/SF). In this method, the FDTD grid is divided into two

\*Address all correspondence to: Ahmed Elmaklizi, E-mail: [ahmed.elmaklizi@ilm.uni-ulm.de](mailto:ahmed.elmaklizi@ilm.uni-ulm.de)

regions (see Fig. 1). The inner region is the total-field region, where the scatterers are located and the fields resulting from the interaction between the scatterers and the incident fields are calculated. In the second region, the scattered-field region, which surrounds the total-field region, only the scattered fields exist. Only the value of the incident field at the boundary between the two regions is needed for the introduction of the incident field into the FDTD grid. This is advantageous since we do not need to store the incident field everywhere in the grid. Thus, it is necessary to calculate an incident field, which is propagating in an arbitrary direction, and then it is possible to store it so that it can be used to update the boundary between the two regions.<sup>13</sup> This is done by propagating and saving a one-dimensional (1-D) wave, and then projecting it on the two-dimensional (2-D) grid. Special care needs to be taken to minimize any numerical dispersion that occurs due to the 1-D wave not coinciding with the simulation rectangular grid for large oblique angles.<sup>13</sup>

The TF/SF method gives the ability to calculate the scattered near fields and to transform these fields to the far-field solution using appropriate near to far-field transformations. The mathematical description of such a transformation has been presented by Taflov and Hagness.<sup>13</sup> In addition, we used a method of averaging the fields based on the geometrical mean to enhance the accuracy.<sup>14</sup>

The TF/SF method also offers the possibility to inject a plane wave at an oblique angle, which is important for the modeling of focused beams in the FDTD method, since it facilitates the modeling of any desired beam as long as we have its ASPW description,<sup>8,9</sup> as will be seen in the next section.

## 2.2 Angular Spectrum of Plane Waves

The main essence of the ASPW method is the usage of the Fourier transform to get the angular spectrum of the beam from its spatial distribution in the focal plane and vice

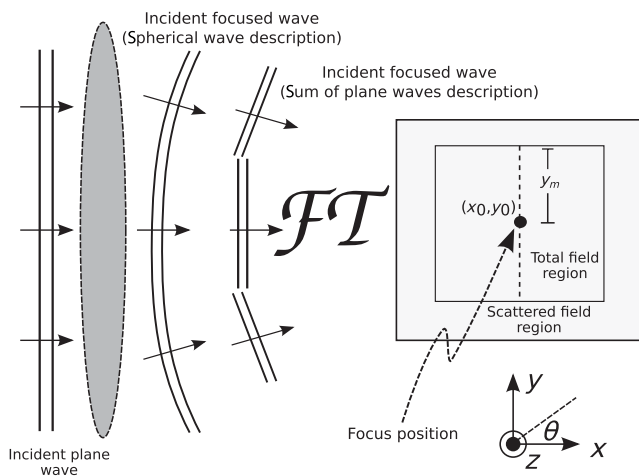


**Fig. 1** The implementation of the angular spectrum of plane waves method in the finite difference time domain (FDTD) method. The plane wave propagates in the  $x$ -direction and passes through a lens where a focused beam is formed at position  $(x_0, y_0)$ . The FDTD grid is divided into a total field region that contains both the incident and the scattered fields and a scattered field region, which contains only the scattered fields. The incoming wave enters the FDTD grid at the interface between total and scattered field.  $y_m$  represents the maximum distance from the focus of the beam to the lateral boundary of the total field and scattered field regions.

versa.<sup>15,16</sup> This allows the modeling of a complicated wave front as a summation of plane waves with different incident angles. The fact that the 2-D case is presented here gives the chance to decouple Maxwell's equations into two independent polarizations, the transverse electric (TE) and the transverse magnetic (TM) polarizations. In this study, only the TM polarization will be discussed since the numerical treatment of both polarizations is identical. Therefore, only the component of the electric field parallel to the  $z$ -axis is regarded, see Fig. 1. For a 2-D setup the electrical fields at position  $(x, y)$  can be realized mathematically as follows:<sup>8</sup>

$$E_{z,m}(x, y) = E_{0,m} \exp[jk(x \cos \theta_m + y \sin \theta_m)] \sqrt{\cos(\theta_m)}. \quad (1)$$

The field  $E_{z,m}$  is the electric field due to a plane wave incident at angle  $\theta_m$ , and  $k$  is the wave number in the surrounding medium. It is related to the wave number in vacuum  $k_0$  according to  $k = nk_0$ , where  $n$  is the refractive index of the medium.  $E_{0,m}$  is the amplitude of the electric field for the  $m$ 'th plane wave.

The superposition of  $M$  plane waves incident from different directions  $\theta_m$  is usually written as an integration over the different incident angles.<sup>15,16</sup> However, in this work, a summation formula is used to model this addition in a discrete form, which is better suited for a numerical solution.<sup>8</sup>

$$E_z(x, y) = \sum_{m=1}^M E_{z,m}(x, y). \quad (2)$$

Taking a constant amplitude for all incident plane waves in the angular domain leads to  $E_{0,m} = E_0$ . By taking the Fourier transform, we find that the  $E_z$  has the distribution of a sinc function in the spatial domain in the focal plane (the dashed line in Fig. 1). This is the definition of the focused beam during this work. A different distribution can be used for the amplitudes which would lead to a different type of beam.

The discretization of the number of plane waves in the ASPW approach places a lower limit for the plane waves number that has to be overcome to achieve proper wave front shaping. This sampling problem has been addressed before in general terms.<sup>9</sup> In a similar approach, the minimum number of plane waves ( $M_{\min}$ ) needed to get a focus with no numerical artifacts due to sampling in the spatial range of size  $(y_m)$ , and for a maximum incident angle  $\theta_{\max}$  (which is the definition for the maximum divergence angle for a focused beam) is found to be

$$M_{\min} = \frac{2y_m \sin(\theta_{\max})}{\lambda} + 1, \quad (3)$$

where  $y_m$  is the maximal distance between the focal point and the simulation grid boundary in  $y$ -direction, see Fig. 1. The first term in the equation is due to sampling theory, whereas the second term takes into account the odd number of plane waves (the wave incident at angle zero). If the number of plane waves used is approximately less than this number, then a distorted image of the beam will appear beside the beam. This is shown numerically in Sec. 3.2.

## 2.3 Beam Scanning (Scattering/Nonscattering Media)

The advantage of having the description of the beam in the ASPW form is the availability of the near fields for every plane wave that is used to propagate the overall beam. This enables us to manipulate the beam in the postprocessing procedure.

In detail, the basic idea of scanning the beam through scattering or nonscattering media is that, by having knowledge about the near fields of the individual plane waves in the steady state, we can produce a shift in the beam focus to an arbitrary position by adding the appropriate phase to the calculated near fields obtained for each plane wave, without the need to perform further simulations. To formulate this idea, Eqs. (1) and (2) are modified to account for the scanning capability:

$$E_{z,\text{shift}}(x, y) = \sum_{m=1}^M E_{z,m}(x, y) \exp[jk(x_{\text{sh}} \cos \theta_m + y_{\text{sh}} \sin \theta_m)], \quad (4)$$

where  $E_{z,\text{shift}}$  is the electric field for a longitudinal shift  $x_{\text{sh}}$  and a lateral shift  $y_{\text{sh}}$  of the focus position.

## 3 Simulation and Results

### 3.1 Verification

For the verification of the implemented FDTD code and the ASPW method, both near and far fields of the light scattered by a single cylindrical scatterer are investigated. First, we present the near fields for the scattering of a plane wave by a cylinder in comparison to the corresponding analytical solution.<sup>12</sup> The wavelength of the incident plane wave is  $1 \mu\text{m}$ , and the refractive index of the cylinder is 1.33, surrounded by air ( $n = 1$ ). The spatial resolution used in the FDTD simulation is equal to  $\lambda/80$ . In Fig. 2, it can be seen that the agreement between the numerical [Fig. 2(a)] and analytical [Fig. 2(b)] results is good. The relative difference between both methods [Fig. 2(c)] is below 1.8%.

Next, the far-field results are verified for several cases. We performed a FDTD simulation for a normally incident plane wave scattered by a cylinder and compared it to the analytical solution.<sup>12</sup> Figure 3 shows the differential scattering cross section for both cases, indicating a good agreement. The maximum and the average relative differences are 7.5% and 1.2%, respectively. Figure 3 shows, in addition, the comparison between the

FDTD simulation for an incident focused beam and the analytical solution. The analytical solution is derived by applying a similar approach as the Fourier Lorenz-Mie theory,<sup>17</sup> where the ASPW method is utilized in the Mie theory to derive an analytical solution of the scattering of a Gaussian beam by a sphere. We used the same technique for an incident focused beam (i.e., a sinc function in the focus) while having a cylindrical scatterer (this solution will be called the Fourier cylinder theory in this article). Again a good agreement between the FDTD results and the analytical solution is obtained, as can be seen in Fig. 3. The maximum and the average relative differences are 14.3% and 2.4%, respectively. We note that these results can be further improved by increasing the spatial resolution of the FDTD grid. In Fig. 3, it can also be seen that the difference between the scattering of light using a plane wave and a focused beam is significant.

### 3.2 Beam Scanning

After examining Eq. (2), it becomes clear that the light in the image plane can be modeled as the superposition of plane waves propagating with different oblique angles. To start the simulation, we use the focused beam ASPW description given in Eq. (1) to get the proper phase for each plane wave. Second step is to propagate the focused beam in time domain through the FDTD grid, and to get the time-averaged steady-state near fields for every plane wave by using a discrete Fourier transform. The next step is to shift the focus through the grid in the steady state. Since all the electric near fields from the individual plane waves are recorded, an extra phase can be added to those of each plane wave according to Eq. (4) in order to shift the focus to the desired position, see Fig. 4. The required position of the focus ( $x_0, y_0$ ) is indicated in the caption of the figure. The intensity of the  $E_z$  component is normalized to the maximum intensity in the beam focus, while the maximum divergence angle of the incident beam is 45 deg.

In Figs. 4(b), 4(d), and 4(e), it can be seen that there is a numerical error in the beam. Distorted images of the original beam are appearing at similar  $x/\lambda$ , but different  $y/\lambda$  positions. These artifacts appear due to the insufficient sampling rate in the angular domain, as has been discussed in Sec. 2.2. In this case, 11-plane waves were used to form the beam. According to Eq. (3), the minimum number of plane waves required to form the beam in this case is 15. It is also interesting to note that when the beam is in the middle of the grid it is sufficient to use a smaller number of plane waves. This is because the

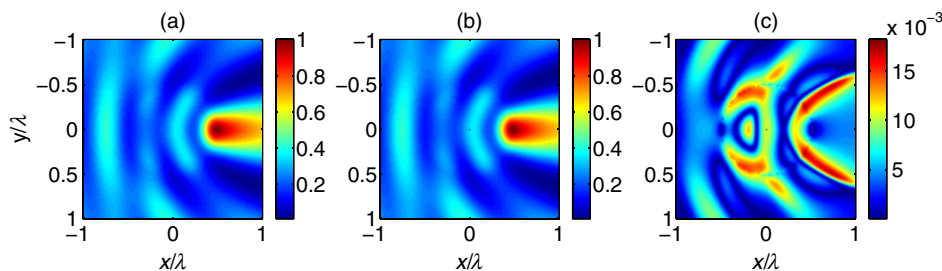


**Fig. 2** Comparison of the normalized intensity of the  $E_z$  component of the electric field for the scattering by a cylinder of diameter  $1 \mu\text{m}$  for an incident plane wave: (a) FDTD simulation, (b) analytical solution, (c) the relative difference between the first two figures. Figures (a) and (b) are normalized to the maximum of the intensity for each case, and the cylinder is located at  $x/\lambda = y/\lambda = 0$ .

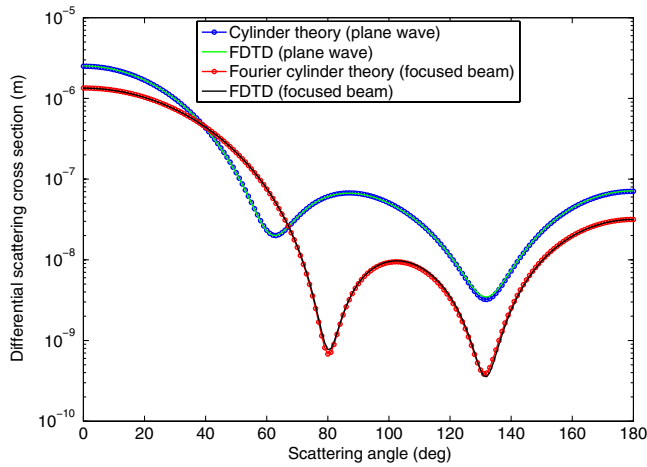


**Fig. 3** The differential scattering cross section of a cylinder with a diameter of  $1 \mu\text{m}$  for an incident plane wave and a focused beam. The focused beam has a maximum divergence angle of  $45^\circ$ , while both the focused beam and the plane wave have the wavelength of  $1 \mu\text{m}$ . The refractive index of the cylinder is  $1.33$  surrounded by air ( $n = 1$ ) in both cases. The spatial resolution in the FDTD simulation is equal to  $\lambda/80$ .

distance between the beam and the more remote lateral boundary of the grid (at  $|y/\lambda| = 5$ ) is smaller in comparison to the case when the beam is closer to one of the lateral boundaries. This can be seen in Fig. 4(a), where only 8-plane waves are required according to Eq. (3), and therefore the 11-plane waves used in this case are sufficient. When the same beam is shifted as in Fig. 4(c), 13-plane waves are needed. And since only 11 are used, a distorted image of the beam appears near a lateral boundary of the grid. In Fig. 5, the number of plane

waves is doubled compared to the results in Fig. 4. Due to this increase, all the numerical artifacts that were shown before have been suppressed.

### 3.3 Scanning Through Scattering Media

In this section, a simulation quite similar to the one performed in the previous section is investigated. However, in this case, the medium is not homogeneous but consists of cylindrical scatterers with refractive index of  $1.45$  suspended in water ( $n = 1.33$ ). The volume concentration of the scatterers is  $30\%$ , which gives a mean free path of  $6.9 \mu\text{m}$  assuming independent scattering. The beam is first scanned in the  $x$ -direction to show the change in the focal shape and intensity in relation to the depth of the precalculated focus of the beam in the sample (Fig. 6). Second, a simulation is presented for the scanning in the  $y$ -direction to show that the same principle works in this case as well (Fig. 7). Also, the intensity of the electric fields that are being shown are not only the incident light, rather they are the intensity of the sum of the incident and the scattered electric fields. We mention this because in Fig. 6, as expected, the focused beam is distorted after propagating through the scatterers. But even before the beam reaches the scatterers, the beam is somehow distorted. This is because of the back-scattered light which interacts with the beam. The intensity in Figs. 6 and 7 is normalized to the maximum intensity of the incident nonscattered focused beam. It can be noticed that in Fig. 6(d), the intensity is increased above 1. This is due to the high constructive interference of the near fields between the two cylinders in the vicinity of the focus. Also, it is interesting to note that the supposed position of the focus diverges from the actual position of the focus especially for the deeper foci. This displacement is partly caused by the different speeds of the beam inside and outside the

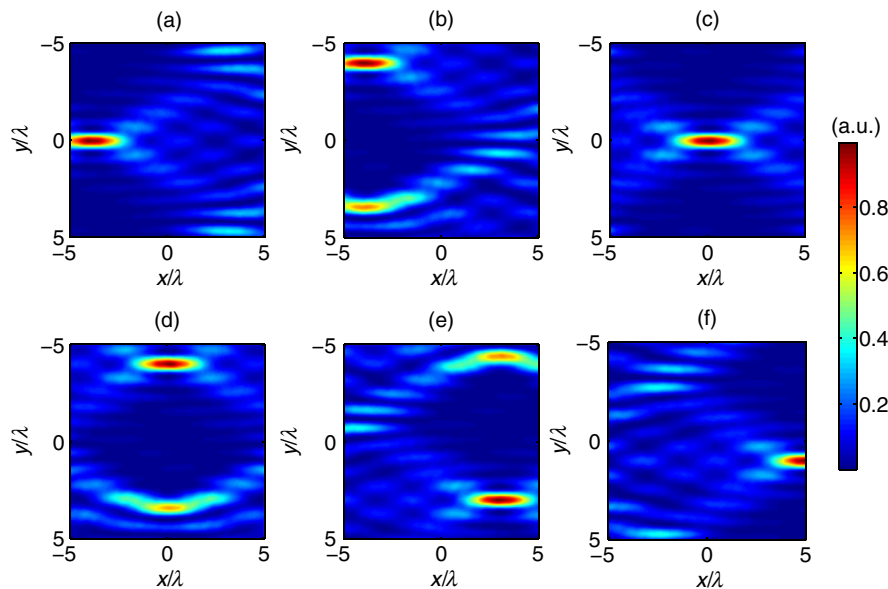


**Fig. 4** The normalized intensity of the  $E_z$  component of the electric field at different positions of the focused beam. The desired focus positions in figures (a) to (f) are at:  $(x_0/\lambda = -4, y_0/\lambda = 0)$ ,  $(x_0/\lambda = -4, y_0/\lambda = -4)$ ,  $(x_0/\lambda = 0, y_0/\lambda = 0)$ ,  $(x_0/\lambda = 0, y_0/\lambda = -4)$ ,  $(x_0/\lambda = 3, y_0/\lambda = 3)$ , and  $(x_0/\lambda = 5, y_0/\lambda = 1)$ . The intensity is normalized to the intensity of the nondisturbed  $E_z$  component at the focus of the beam. 11 plane waves are used to form the focused beam. The maximum divergence angle is  $45^\circ$  and the wavelength of the incident light is  $1 \mu\text{m}$ . The spatial resolution in the FDTD simulation is equal to  $\lambda/20$ .

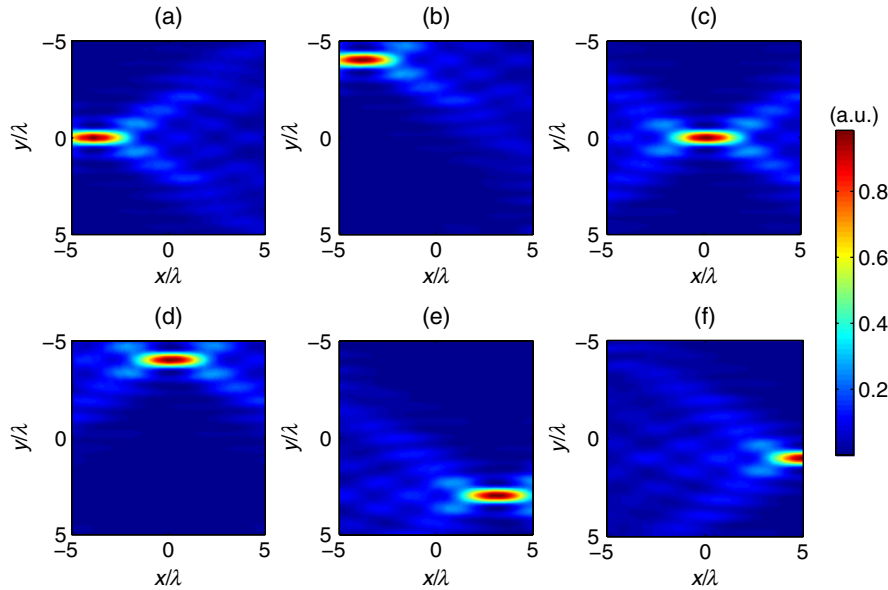


**Fig. 5** The normalized intensity of the  $E_z$  component of the electric field at different positions of the focused beam. The desired focus positions in the figures (a) to (f) are at:  $(x_0/\lambda = -4, y_0/\lambda = 0)$ ,  $(x_0/\lambda = -4, y_0/\lambda = -4)$ ,  $(x_0/\lambda = 0, y_0/\lambda = 0)$ ,  $(x_0/\lambda = 0, y_0/\lambda = -4)$ ,  $(x_0/\lambda = -3, y_0/\lambda = 3)$ , and  $(x_0/\lambda = 5, y_0/\lambda = 1)$ . The intensity is normalized to the intensity of the nondisturbed  $E_z$  component at the focus of the beam. Twenty-one plane waves are used to form the focused beam. The maximum divergence angle is 45 deg and the wavelength of the incident light is  $1 \mu\text{m}$ . The spatial resolution in the FDTD simulation is equal to  $\lambda/20$ .

scatterers since the expected focus positions are calculated with the assumption of no scattering. By examining Fig. 6, it becomes apparent that the deeper the light propagates through the sample, the more the intensity of the focus decreases and its shape is distorted. More precisely, the relative width of the beam is enlarged and, in addition, further unintentional “foci” due to

interference of scattered light appear at larger depths of the precalculated focus position. We note that to reach these conclusions, it was necessary to run the simulation for more realizations of the scatterers’ positions (figure not shown).

The simulations presented in Fig. 6 were allocated a memory of 47.3 Mbyte, compared to 2.25 Mbyte, which is needed to

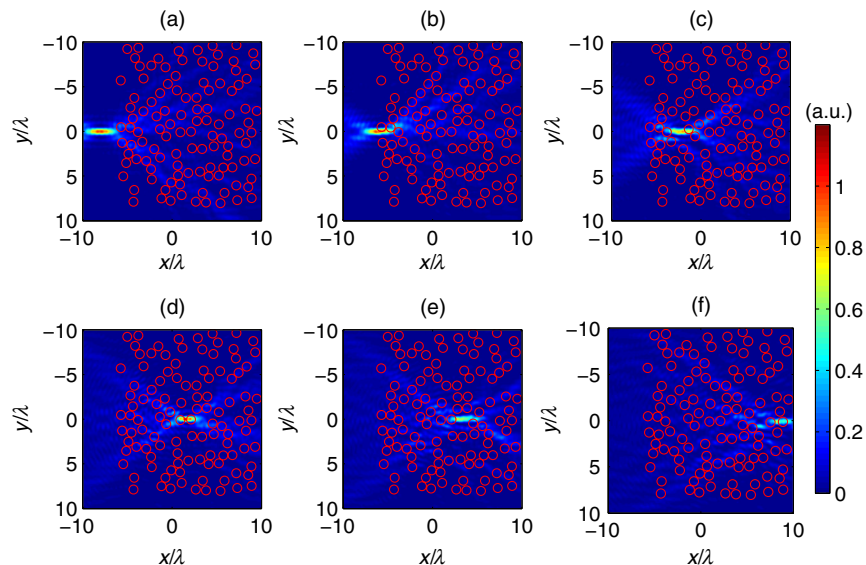


**Fig. 6** The normalized intensity of the  $E_z$  component of the electric field for axial scanning ( $x$ -direction) at  $y_0 = 0$ . The normalization is relative to the maximum intensity of the incident nonscattered focused beam. The figures from (a) to (f) show focus positions at:  $(x_0/\lambda = -8, y_0/\lambda = 0)$ ,  $(x_0/\lambda = -6, y_0/\lambda = 0)$ ,  $(x_0/\lambda = -2, y_0/\lambda = 0)$ ,  $(x_0/\lambda = 2, y_0/\lambda = 0)$ ,  $(x_0/\lambda = 4, y_0/\lambda = 0)$ , and  $(x_0/\lambda = 9, y_0/\lambda = 0)$ . Twenty-one plane waves are used to form the beam. The scatterers are cylinders with refractive index of 1.45, while the surrounding medium has a refractive index of 1.33. The wavelength of the incident light is  $1 \mu\text{m}$  and the maximum divergence angle of the focused beam is 45 deg. The spatial resolution in the FDTD simulation is equal to  $\lambda/20$ .

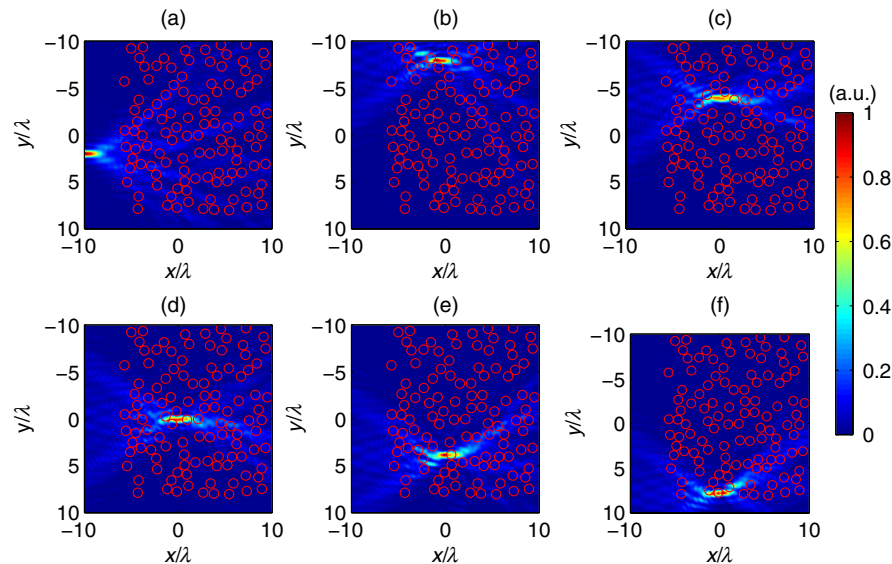


**Fig. 7** The normalized intensity of the  $E_z$  component of the electric field for lateral scanning ( $y$ -direction) at  $x_0 = 0$ . The normalization is relative to the maximum intensity of the incident nonscattered focused beam. The figures from (a) to (f) show focus positions at:  $(x_0/\lambda = -10, y_0/\lambda = 2)$ ,  $(x_0/\lambda = 0, y_0/\lambda = -8)$ ,  $(x_0/\lambda = 0, y_0/\lambda = -4)$ ,  $(x_0/\lambda = 0, y_0/\lambda = 0)$ ,  $(x_0/\lambda = 0, y_0/\lambda = -4)$ , and  $(x_0/\lambda = 0, y_0/\lambda = 8)$ . Twenty-one plane waves are used to form the beam. The scatterers are cylinders with refractive index of 1.45, while the surrounding medium has a refractive index of 1.33. The wavelength of the incident light is  $1 \mu\text{m}$ , and the maximum divergence angle of the focused beam is  $45 \text{ deg}$ . The spatial resolution in the FDTD simulation is equal to  $\lambda/20$ .

save the data in a classical FDTD simulation. In return, the simulation took  $\sim 40$  min compared to 14 h, which is the time needed for a classical FDTD simulation.

#### 4 Conclusion and Discussion

In this work, a highly efficient method of simulating the scanning of a focused beam through scattering (or nonscattering) media is presented. For simulating the near fields in scattering media caused by an incident focused beam, the calculation of the near fields of several ( $M$ ) plane waves incident at different angles relative to the optical axis is needed, see Eq. (2). Further, if the near fields caused by a beam focused at any other position is searched for, the already calculated near fields due to the  $M$ -plane waves can be used. The only difference is that the near fields have to be modified simply by adding the phases given in Eq. (4) to every plane wave. This method avoids the need to run the simulation for every focus position. Similarly, the near fields for the  $M$ -plane waves calculated with the FDTD method can be used to obtain the near fields for a focused beam having an arbitrary intensity profile, for example of a Gaussian profile. This is achieved by changing the amplitude of the near fields caused by the  $M$ -plane waves.

A MATLAB code was developed for the FDTD simulation tool to implement the focused beam using the ASPW description. The code was verified for both the near and far fields by comparison with analytical solutions for both an incident plane wave and an incident focused beam. Due to the high computational power needed to run the FDTD code, the simulations shown were performed in two dimensions. However, the method developed can be easily used in three-dimensional (3-D) cases since the only difference is the need to take the TE and TM polarization simultaneously into account since it will not be possible to decouple them anymore. We note that 3-D simulations

necessitate, in principle, higher demands on the computer memory for each incident plane wave compared to 2-D simulations and, in addition, more plane waves are usually needed to form the desired beam. However, for many cases, one is only interested in the results in a restricted spatial region of the simulation area. Thus, only the fields in that region have to be stored, which strongly reduces the memory demands. The developed method is very powerful for the study of the optimization of the beam focus in scattering media, especially since in that case, it will only be necessary to store the data in the region where we are trying to optimize the focus as was mentioned before.

The presented work is a capable tool to further study scanning microscopes since in a typical experiment, the beam is scanned over 256 points in every direction which gives around 16-million scanning points with equal number of simulation runs. Using the presented method, the scanning can be simulated in a single run followed by a simple and fast postprocessing algorithm. Thus, the simulation time is reduced by more than 7 orders of magnitude compared to the current state-of-the-art techniques. This enhancement in speed can be highly beneficial for developing new techniques for beam scanning through biological tissue and the suppression of the focus degradation even after multiple scattering events, which is important for biological tissue studies.

#### References

1. J. M. Schmitt, A. Knüttel, and M. Yadlowsky, "Confocal microscopy in turbid media," *J. Opt. Soc. Am. A* **11**(8), 2226–2235 (1994).
2. W. Denk, J. H. Strickler, and W. W. Webb, "Two-photon laser scanning fluorescence microscopy," *Science* **248**(4951), 73–76 (1990).
3. D. Roy, "Two-photon scattering of a tightly focused weak light beam from a small atomic ensemble: an optical probe to detect atomic level structures," *Phys. Rev. A* **87**(6), 063819 (2013).

4. A. Knüttel, S. Bonev, and W. Knaak, "New method for evaluation of in vivo scattering and refractive index properties obtained with optical coherence tomography," *J. Biomed. Opt.* **9**(2), 265–273 (2004).
5. I. M. Vellekoop and A. P. Mosk, "Focusing coherent light through opaque strongly scattering media," *Opt. Lett.* **32**(16), 2309–2311 (2007).
6. I. M. Vellekoop and A. P. Mosk, "Phase control algorithms for focusing light through turbid media," *Opt. Commun.* **281**(11), 3071–3080 (2008).
7. X. Yang et al., "Three-dimensional scanning microscopy through thin turbid media," *J. Opt. Soc. Am.* **20**(3), 2500–2506 (2012).
8. I. R. Çapoğlu, A. Taflove, and V. Backman, "Generation of an incident focused light pulse in FDTD," *Opt. Express* **16**(23), 19208–19220 (2008).
9. I. R. Çapoğlu, A. Taflove, and V. Backman, "Computation of tightly-focused laser beams in the FDTD method," *Opt. Express* **21**(1), 87–101 (2013).
10. M. S. Starosta and A. K. Dunn, "Three-dimensional computation of focused beam propagation through multiple biological cells," *Opt. Express* **17**(15), 12455–12469 (2009).
11. R. L. Coe and E. J. Seibel, "Computational modeling of optical projection tomographic microscopy using the finite difference time domain method," *J. Opt. Soc. Am. A* **29**(12), 2696–2707 (2012).
12. C. F. Bohren and D. R. Huffman, *Absorption and Scattering of Light by Small Particles*, Wiley Science Paperback Series, Chichester, UK (1998).
13. A. Taflove and S. C. Hagness, *Computational Electrodynamics: The Finite-Difference Time-Domain Method*, Artech House, Norwood (2005).
14. D. J. Robinson and J. B. Schneider, "On the use of the geometric mean in FDTD near-to-far-field transformations," *IEEE Trans. Antennas Propag.* **55**(11), 3204–3211 (2007).
15. S. Kozaki, "Scattering of a gaussian beam by a homogeneous dielectric cylinder," *J. Appl. Phys.* **53**(11), 7195–7200 (1982).
16. J. W. Goodman, *Introduction to Fourier Optics*, McGraw-Hill, New York (1968).
17. E. E. M. Khaled, S. C. Hill, and P. W. Barber, "Scattered and internal intensity of a sphere illuminated with a gaussian beam," *IEEE Trans. Antennas Propag.* **41**(3), 295–303 (1993).

**Ahmed Elmaklizi** is a PhD student at the Institut für Lasertechnologien in der Medizin und Meßtechnik (ILM), Ulm, Germany, and part of the "Materials Optics and Imaging" group at ILM. He got his BSc degree in electrical engineering from the German University in Cairo (GUC), and got his master of science degree in communication engineering from University of Ulm.

**Jan Schäfer** has worked for nine years in the "Materials Optics and Imaging" group of Professor Kienle at the Institut für Lasertechnologien in der Medizin und Meßtechnik (ILM), Ulm, Germany. He studied mathematics and investigated different methods to numerically and analytically solve Maxwell's equations for biomedical purposes during his doctoral thesis and PhD work at the ILM. At the moment he is working as a software architect for an automotive supplier.

**Alwin Kienle** is vice director (Science) of the Institut für Lasertechnologien in der Medizin und Meßtechnik (ILM), Ulm, Germany, and head of the "Materials Optics and Imaging" group at ILM. In addition, he is a professor at the University of Ulm. He studied physics and received his doctoral and habilitation degrees from University of Ulm. As post-doc he worked with research groups in Hamilton, Canada, and in Lausanne, Switzerland.